Tetrahedron 67 (2011) 4009–4016

Contents lists available at ScienceDirect

Tetrahedron

journal homepage: www.elsevier.com/locate/tet

Novel tetradentate chelators derived from 3-hydroxy-4-pyridinone units: synthesis, characterization and aqueous solution properties

Andreia Leite [a], Ana M.G. Silva [a], Ana Nunes [a], Mariana Andrade [a], Carla Sousa [b], Luís Cunha-Silva [a], Paula Gameiro [a], Baltazar de Castro [a], Maria Rangel [c,*]

[a] REQUIMTE, Departamento de Química e Bioquímica, Faculdade de Ciências, Universidade do Porto, 4169-007 Porto, Portugal
[b] REQUIMTE, Faculdade de Ciências da Saúde, Universidade Fernando Pessoa, Rua Carlos da Maia, 4200-150 Porto, Portugal
[c] REQUIMTE, Instituto de Ciências Biomédicas Abel Salazar, 4099-003 Porto, Portugal

ARTICLE INFO

Article history:
Received 8 February 2011
Received in revised form 29 March 2011
Accepted 11 April 2011
Available online 16 April 2011

Keywords:
3-Hydroxy-4-pyridinone ligands
Tetradentate chelators
Acid–base properties

ABSTRACT

The synthesis and characterization of three novel tetradentate ligands (**T1**, **T2** and **T3**) based on 3-hydroxy-4-pyridinone chelating units are described. The three ligands exhibit different flexibility due to the use of two different anchor molecules, piperazine and 1,2-diaminobenzene, and to the diverse length of the 3-hydroxy-4-pyridinone arms. All reactions were performed using both conventional heating and microwave irradiation in order to evaluate the possibility of using greener methods in these synthetic procedures. The results showed that, in all cases, microwave irradiation provides the desired ligands reducing reaction time in ca. 97%. The structure of ligand **T3** was resolved by X-ray crystallography, showing significant hydrogen bonding and interesting π–π interaction between the benzene and pyridinone rings. The use of potentiometric and spectroscopic methods allowed determination of acidity constants and unequivocal assignment of proton loss for each pK_a value. Interaction of the ligands with divalent metal ions was assessed by spectroscopic methods.

1. Introduction

Ligands of the 3-hydroxy-4-pyridinone (3,4-HPO) type are well known for their biomedical, chemical and analytical applications. The possibility of using these ligands in such a variety of fields is mainly due to their high affinity towards M(II) and M(III) metal ions as well as their versatility in synthesis.[1]

In the recent years, a significant number of these bidentate ligands with variable lipophilicity have been prepared and used to produce tetra and hexadentate chelators. These polydentate ligands originate metal ion complexes with different thermodynamic and kinetic properties thus allowing a better choice for its use. Also, additional functionalities such as fluorophores[2] and anchoring molecules,[3] to connect the ligands to surfaces or polymers, have been successfully introduced thus enlarging their range of application.

Several cyclic and acyclic backbones functionalized with pendant arms have been used to prepare hydroxypyridinone derivatives, namely platforms including the six-membered heterocyclic piperazine backbone to anchor 3,2-HPO chelating unities with the purpose of preparing siderophore mimics.[4] In the latter and other related examples,[5] the piperazine molecule has been used as a backbone in supramolecular coordination chemistry and in the preparation of several coordination polymers.[6] Acyclic backbones such as amino-triscarboxylic anchoring skeletons, were also used in the synthesis of tripodal tris(3-hydroxy-4-pyridinone) hexadentate chelators.[7]

As part of an on-going project focused on the preparation of 3-hydroxy-4-pyridinone complexes of vanadium(IV) and zinc(II) with potential as insulin enhancing agents, we designed tetradentate ligands based on 3,4-HPO bidentate units in order to compare the activity of complexes with different stability and lability. In this work we report the preparation of three novel tetradentate 3,4-HPO chelators, which exhibit different flexibility due to the use of two anchor molecules, piperazine and 1,2-diaminobenzene, and diverse length of the 3-hydroxy-4-pyridinone arms.

In a first approach, 1,4-bis(3-aminopropyl)piperazine was chosen to anchor the two 3,4-HPO units since this platform can provide the required flexibility for metal ion chelation and enhance solubility in water due to the presence the two extra amine groups. The two primary nitrogen atoms of the piperazine side-arms can easily be linked to the 3,4-HPO chelating unities through (i) a direct condensation reaction allowing the formation of the ligand **T1** (Fig. 1) or (ii) an amide linkage allowing the synthesis of the ligand **T2** (Fig. 1). The results obtained show that these ligands differ both in their overall molecular shape and in

* Corresponding author. E-mail address: mcrangel@fc.up.pt (M. Rangel).

0040-4020/$ – see front matter © 2011 Elsevier Ltd. All rights reserved.
doi:10.1016/j.tet.2011.04.035

flexibility. As a drawback, the piperazine scaffold introduces two additional heterocyclic nitrogen atoms, which contribute to the acid–base properties of the ligands giving rise to a higher number of equilibria in aqueous solution and in the presence of metal ions. In order to overcome this problem we used a different anchoring molecule, 1,2-diaminobenzene and synthesized ligand **T3** (Fig. 1). This platform also provides a relatively rigid and hindered structure to anchor the chelating units. The different structure of the two platforms is reflected in the structure of ligands **T1**, **T2** and **T3** and that of the corresponding metal ion complexes.

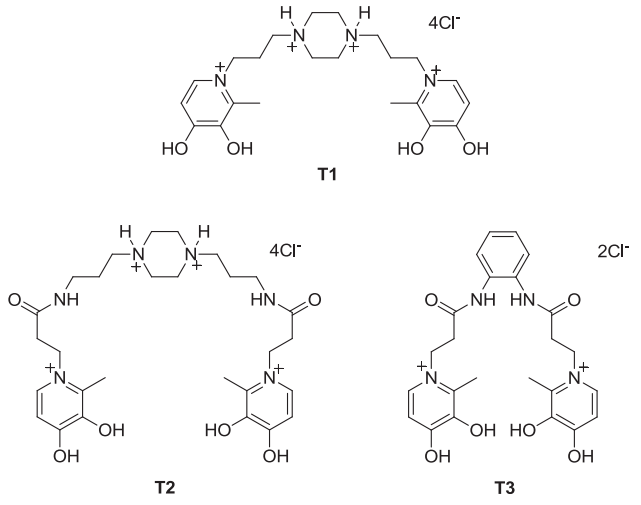

Fig. 1. Ligands **T1**, **T2** and **T3** described in the present work.

The acid–base properties of the three ligands were examined in aqueous solution by using potentiometric and spectrophotometric methods. The values of the acidity constants of the ligands were calculated from titration data and unequivocal assignment of proton loss for each pK_a value was assessed by NMR. Interaction of the ligands with divalent metal ions was assessed by spectroscopic methods.

2. Results/discussion

2.1. Synthesis and characterization

Scheme 1 outlines the synthesis of tetradentate 3,4-HPO ligands **T1** and **T2** bearing the same 1,4-bis(3-aminopropyl)piperazine scaffold and different side-arms; the protected form of **T1** (derivative **1**) arises from the direct condensation of piperazine with 3-benzyloxy-2-methyl-4-pyrone, whereas the protected form of **T2** (derivative **2**) arises from the amide coupling of piperazine with 3-benzyloxy-1-(3′-carboxypropyl)-2-methyl-4-pyridinone. Thus, to synthesize **2** a solution of 3-benzyloxy-2-methyl-4-pyrone and 1,4-bis(3-aminopropyl)piperazine, in a mixture of ethanol, water and NaOH, was refluxed for 24 h, affording the corresponding bis-condensation derivative **1** in 70% yield. The synthesis of derivative **2** involves a coupling step of 3-benzyloxy-1-(3′-carboxypropyl)-2-methyl-4-pyridinone with 1,4-bis(3-aminopropyl)piperazine, using DCC (*N*,*N*′-dicyclohexylcarbodiimide) and HOBt (1-hydroxybenzotriazole) as coupling agents, at room temperature for 4 days. After purification by column chromatography, the expected derivative **2** was obtained in 65% yield.

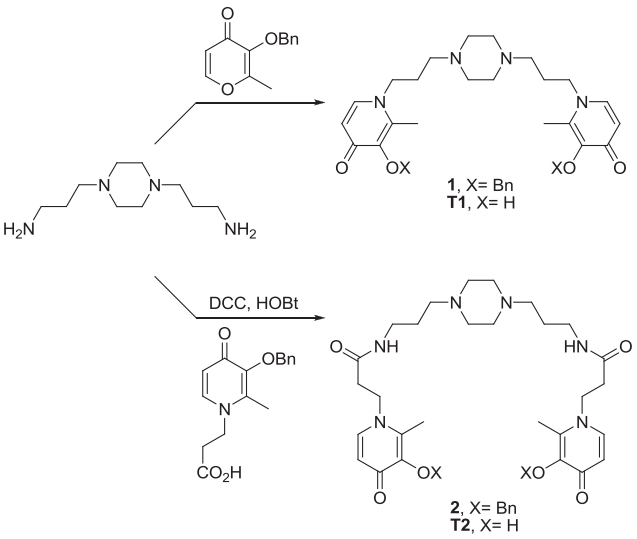

Scheme 1. Synthesis of ligands **T1** and **T2**.

Derivative **3** (Scheme 2) was prepared in 31% yield from the reaction of 3-benzyloxy-1-(3′-carboxypropyl)-2-methyl-4-pyridinone with 1,2-diaminobenzene, in the presence of DCC and HOBt (room temperature, 3 days) using the same synthetic methodology.

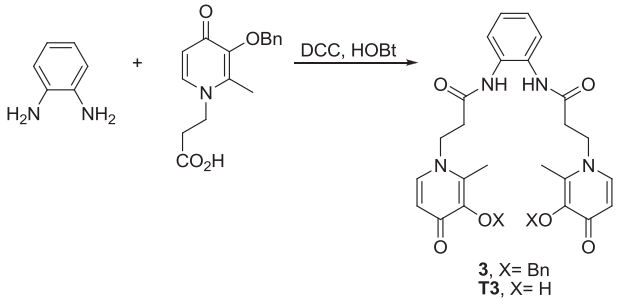

Scheme 2. Synthesis of ligand **T3**.

Subsequent removal of the benzyl protecting groups using a solution of BCl_3 in dichloromethane, lead to the desired hydrochloride salt of ligands **T1**, **T2** and **T3** in good yields.

The latter synthetic protocols proved to be simple and easy to perform but the reactions are quite slow and therefore very time consuming. In order to improve the reaction rates, controlled single-mode microwave heating was tested as opposed to the traditional heating. Microwave irradiation has become a very popular technique that provides a direct and rapid heating with a very high energetic efficiency.[8] A significant number of synthetic reactions have been improved by microwave irradiation, including the synthesis of ligands with different denticities.[9] In many examples reported in the literature, microwave heating dramatically reduced reaction times, in some cases increased reaction yields, and enhanced product purity by reducing unwanted side-reactions compared with conventional heating methods. In the present work, the use of microwave heating significantly diminished reaction times in such a way that derivatives **1**, **2** and **3** were prepared in 30 min and at 50 °C, opposed to 24 h and 80 °C for derivative **1**, 4 days and room temperature for derivative **2** and 3 days and room temperature for derivative **3**.

2.2. NMR spectroscopy

The ^{1}H NMR spectra of derivatives **1**, **2** and **3** are relatively simple, which reflects the symmetry of the compounds. From the

analysis of ^{1}H NMR spectra of these precursors, one can detect that the most characteristic signal or group of signals of the common structural feature, which is the 3,4-HPO ring, are two doublets corresponding to the resonance of 5-H and 6-H protons. The resonance of 6-H appears at higher frequencies (δ=7.58, 7.51 and 7.61 ppm, respectively, in **1**, **2** and **3**) than those corresponding to 5-H (δ=6.13, 6.11 and 6.15 ppm, respectively, in **1**, **2** and **3**). This fact is due to the mesomeric and anisotropic deshielding effect of the carbonyl group in 6-H. Another important feature is the presence of the NH resonance signal from the amide linkage present in derivatives **2** and **3**, which appear as a triplet at δ 7.96 ppm in **2** and as a singlet at δ 9.41 ppm in **3**. When the benzyl groups are removed from these derivatives using BCl_3 protocol, the resulting ligands **T1**, **T2** and **T3** are isolated as hydrochloride salts, in the dihydroxypyridinium form. This is elucidated by the absence of the resonance of the benzyl groups and by the resonances of 6-H and 5-H protons, which undergo downfield shifts. Indeed, 6-H appears at δ 7.93, 7.97 and 8.28 ppm, respectively, in **T1**, **T2** and **T3**, and 5-H appears at δ 6.70, 7.04 and 7.31 ppm, respectively, in **T1**, **T2** and **T3**. These chemical shifts values are in agreement with chemical shifts values found for other related (3,4-HPO)s isolated in the dihydroxypyridinium form.[9b]

2.3. X-ray crystallography

Crystalline material of ligand **T3** suitable for single-crystal X-ray diffraction analysis was obtained by controlled recrystallization from a mixture of dichloromethane/*n*-hexane. Unfortunately, it has not been possible to isolate crystals of ligands **T1** and **T2** with quality for X-ray diffraction methods, although many attempts and distinct procedures have been carried out. The crystal structure of **T3** was determined in the monoclinic crystal system and in the centrosymmetric space group $P2_1/n$, confirming that the ligand **T3** was isolated as hydrochloride salts in dihydroxypyridinium form (Fig. 2). The asymmetric unit cell (asu) includes one cationic ligand **T3**, two chloride anions and, three water molecules and half *n*-hexane molecule, as crystallization solvents (more details related with the crystallographic data collection and structure refinement are in Experimental section). Ligand **T3** shows a structural arrangement with the two 3,4-HPO moieties practically parallel, since the dihedral angle between both the planes defined by these groups is only 4.210°. The 3,4-HPO units are considerably twisted with respect to the phenyl ring of the 1,2-diaminobenzene anchor group (the dihedral angles between the planes of each 3,4-HPO moiety and the phenyl ring are ca. 66.633° and 70.821°).

The structural conformation of ligand **T3** is definitely conditioned and stabilized by an extensive network of inter-molecular interaction, mainly hydrogen bonds and π···π stacking. Adjacent molecules interact directly by π···π contacts involving two pyridinone rings (green shadow in Fig. 3a) and a pyridinone unit with the benzene ring (yellow shadow in Fig. 3a) with the $C_g\cdots C_g$ distances of 3.5264(2) Å and 3.7763(2) Å, respectively (C_g represents the gravity centre of the ring). Furthermore, the ligands **T3** are involved in an extensive inter-molecular hydrogen bonding network with the crystallization water molecules, O–H···O and N–H···O interactions, as well with the chloride anions, O–H···Cl and N–H···Cl interactions, with distances D–H···A found between 1.684(16) and 2.465(11) Å (ligh-blue dashed lines in Fig. 3b; for geometric details about hydrogen bounds see Table S1 in Supplementary data). In this cooperative hydrogen bonding network, the organic molecules act principally as donor, through the hydroxyl groups of pyridinone rings [O(2)–H(7)···O(4)^{i}; O(3)–H(8)···O(3W); O(5)–H(9)···Cl(2)^{ii} and O(6)–H(12)···O(2W); symmetry operations: (i) $-x+3, -y, -z$ and (ii) $x, y, z+1$] and the amine group [N(1)–H(1)···Cl(1) and N(2)–H(6)···O(1W)]. Interestingly, the hydrogen bond interactions between the crystallization waters and the chloride counterions [O(1W)–H(1W)···Cl(2)^{iii}; O(1W)–H(2W)···Cl(1)^{iii}; O(2W)–H(3W)···Cl(1)^{iv} and O(3W)–H(5W)···Cl(2)^{v}; symmetry operations: (iii) $x+1/2, -y+1/2, z+1/2$; (iv) $x-1/2,$

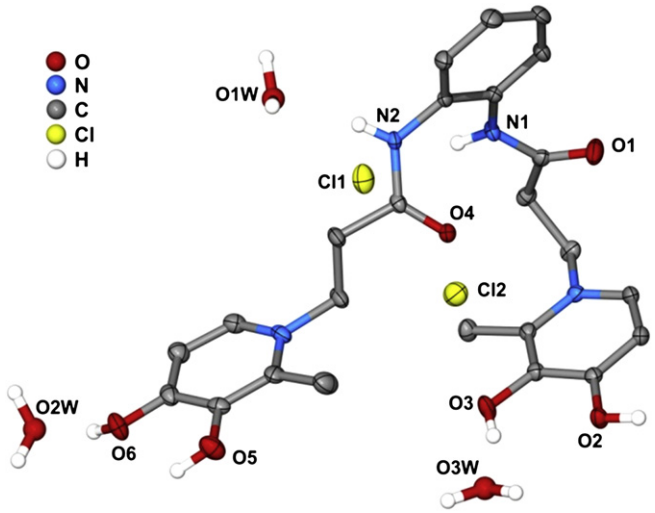

Fig. 2. Crystalline structure of the ligand **T3**, with three crystallization water molecules and two chloride ions, showing the labelling scheme for selected atoms; ellipsoids were drawn at the 50% probability level and hydrogen bonded to carbon atoms have been omitted for clarity purposes.

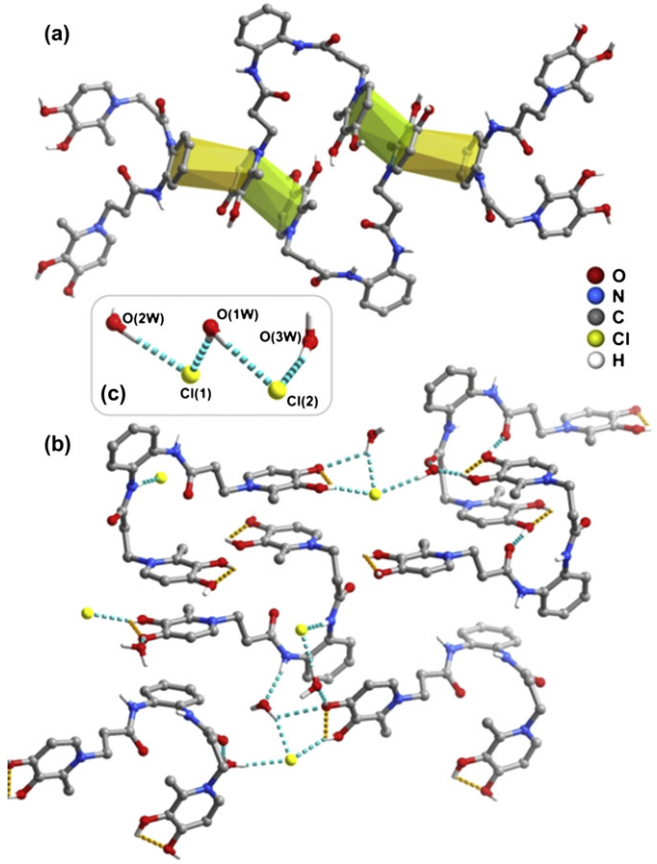

Fig. 3. Non-covalent interactions: (a) π···π stacking involving pyridinone–pyridinone rings (green shadow) and pyridinone–benzene rings (yellow shadow) of adjacent ligands **T3**; (b) hydrogen bonding network, where the light-blue and the orange dashed lines represent inter- and intra-molecular interactions, respectively; (c) the pentameric hydrogen bounded cluster with three water molecules and two chloride anions.

−y+1/2, z+1/2 and (v) −x+2, −y, −z.] lead to the formation of a pentameric cluster that include three water molecules and two chloride anions (Fig. 3b). Additionally, intra-molecular O–H···O hydrogen bonds were observed between the adjacent hydroxyl groups belonging to the same pyridinone ring (orange dashed lines in Fig. 3b). Ultimately, all the inter-molecular interactions lead to the formation of a 3D supramolecular network (not shown). The extended packing of ligand **T3** in the [100] direction of the unit cell shows apertures, which house the charge-balancing chloride as well as the crystallization water and n-hexane molecules (Fig. S1).

2.4. Characterization in aqueous solution

The acidity constants of **T1**, **T2** and **T3** were calculated from potentiometric and UV–vis spectroscopy data and the values obtained are reported in Table 1 together with those of 1,2-dimethyl-3-hydroxypyridinone (Hdmpp) and piperazine for comparison.

Table 1
Acidity constants of ligands **T1**, **T2**, **T3**, Hdmpp and piperazine

pK_{ai}	T1 pot	T2 pot	T2 UV–vis	T3 pot	T3 UV–vis	Hdmpp[a] pot	Piperazine[b] pot
pK_{a1}	2.26±0.10	2.28±0.02	2.35±0.36	3.00 ±0.04	2.78±0.14	3.69±0.01	5.64
pKa_2	2.96±0.06	3.07±0.10	2.67±0.26	3.14 ±0.02	3.42±0.17	9.61±0.03	9.82
pK_{a3}	3.47±0.07	3.40±0.08	3.24±0.43	8.77±0.14	8.17±0.18	—	—
pK_{a4}	6.76±0.08	7.14±0.10	7.17±0.50	9.86±0.07	9.99±0.18	—	—
pK_{a5}	9.10±0.08	9.14±0.10	8.14±0.22	—	—	—	—
pK_{a6}	9.80±0.08	9.70±0.19	9.58±0.11	—	—	—	—

[a] Ref. 10.
[b] Ref. 5.

The acidity constants of ligand **T2** were determined both by potentiometric and spectrophotometric methods and values obtained are in good agreement for the two methods. Due to the low solubility in water of ligands **T1** and **T3** the corresponding values of acidity constants were obtained by UV–vis spectroscopy.

Isolated in the dihydroxypyridinium form, ligand **T3** possesses four dissociable protons, which correspond to the two hydroxyl groups of the two pyridinone rings. The first two constants (pK_{a1} and pK_{a2}) can be related to the deprotonation of the oxygen atom on the pyridinone ring. The remaining two constants (pK_{a3} and pK_{a4}) are assigned to the deprotonation of the enolate group of the pyridinone. These values are in close agreement with the previously reported for Hdmpp.

Regarding ligands **T1** and **T2**, also isolated in the dihydroxypyridinium form, there are two additional acidity constants resulting from the piperazine ring. Typical piperazine acidity constants are 5.64 and 9.82 and the difference between these two values is due to the electrostatic repulsion between the protonated atoms of the piperazine ring.[5]

The deprotonation sequence of **T2** has been assessed on the basis of the pH dependence of the ^{1}H NMR chemical shifts over the range 1.96–11.11 at 25 °C of the non-labile protons and is presented in Scheme 3. In the pH range 1.96–4.00 (see selected spectra in Fig. 4) the signals of both aromatic protons of the pyridinone ring are significantly shifted to lower values of chemical shift, while the signals of the remaining protons are slightly adjusted. These data indicate that the pK_{a1} and pK_{a2} values can be associated with the first deprotonation of the two pyridinone rings. In pH ranges from 4.00–4.71 to 7.56–8.14 the aliphatic protons of the piperazine ring together with those of H-11 and H-16 are significantly shifted to lower values of chemical shift, whereas the peaks corresponding to the remaining protons are not perturbed. These results reveal that the pK_{a3} and pK_{a4} values are associated with the deprotonation of the first and the second nitrogen atoms of the piperazine ring. At higher pH values (above 9.00) the deprotonation of the enolate group of the two pyridinone rings is observed giving rise to pK_{a5} and pK_{a6}.

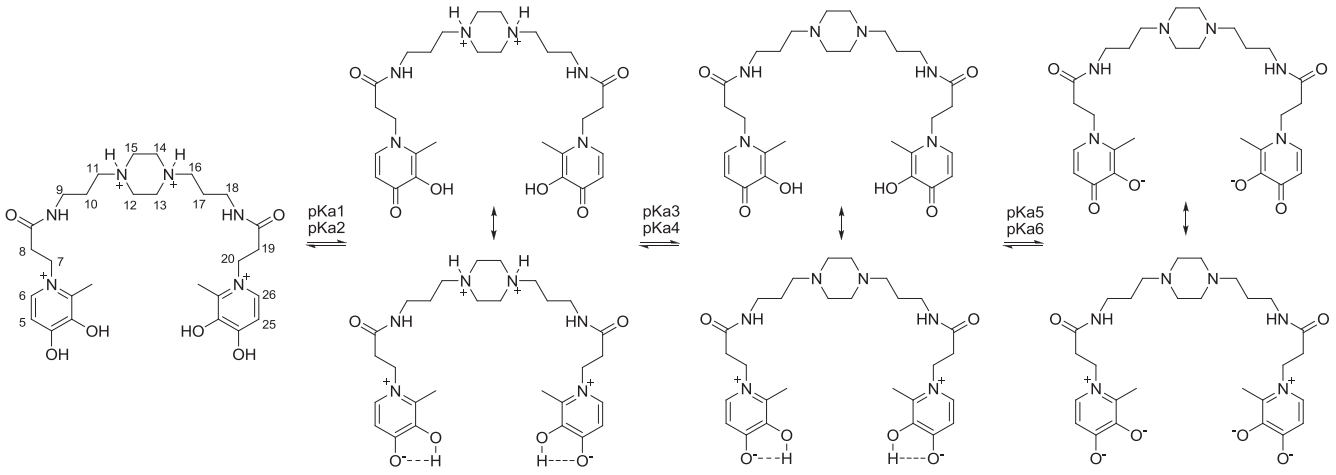

Scheme 3. Dissociation steps of ligand **T2**.

The distribution diagrams as a function of pH of the ligands are available in Supplementary data. The distribution diagrams clearly illustrate the different number of species that result in each case and allow identification of the predominant species at physiological pH.

2.5. Coordination with VO(II), Zn(II) and Cu(II)

The interaction of ligands **T1**, **T2** and **T3** with divalent metal ions was investigated for VO(II), Zn(II) and Cu(II) by mixing the

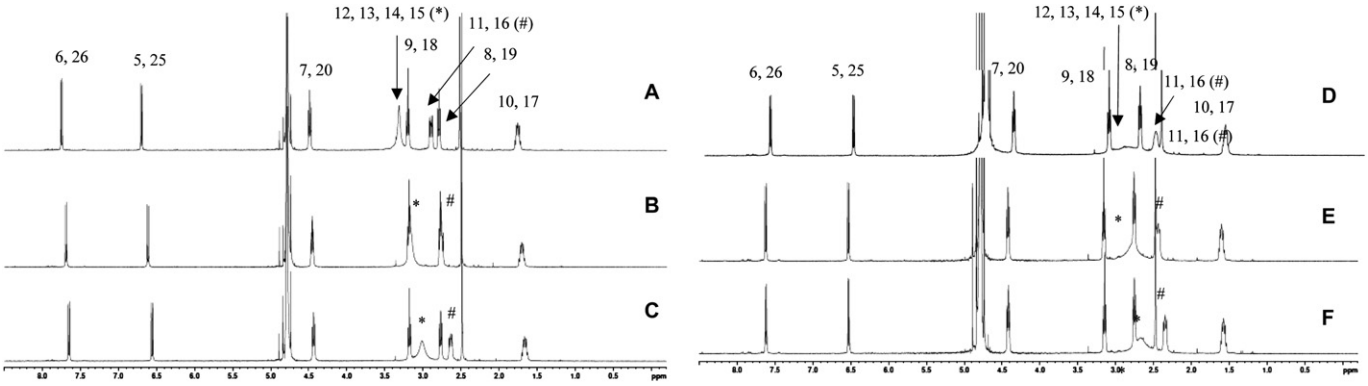

Fig. 4. ^{1}H NMR spectra (spectrum A: pH=3.43; spectrum B: pH=4.00; spectrum C: pH=4.71; spectrum D: pH=7.20; spectrum E: pH=7.56; spectrum F: pH=8.14) of the ligand **T2**.

appropriate reagents to prepare the corresponding metal complexes according to the usual procedures for 3,4-HPO ligands.[11] Formation of complexes was detected visually for ligands **T1** and **T3** since immediate precipitation occurred in contrast with ligand **T2** for which complexes were more difficult to isolate as powders. Evidence for the formation of complexes in solution was provided for zinc(II) by the characteristic deviation of ca. 1 ppm in the ^{1}H NMR chemical shifts of protons H5 and H6 of the pyridinone ring (Scheme 3) and a bathochromic shift of ca. 30 nm in the UV–vis spectra (Figs. S1 and S2 in Supplementary data) and for oxidovanadium(IV) complexes by the observation of the characteristic UV–vis spectra (Fig. S3 in Supplementary data).[12] Interaction of copper(II) with the three ligands was assessed by EPR spectroscopy and the results obtained are shown in Fig. 5.

The EPR spectra depicted in Fig. 5 show the typical signal of copper(II) complexes in the g=2 region and exhibit for ligands **T1** and **T2** an additional signal at g=4. The latter is better resolved for **T2** and clearly shows the hyperfine interaction of the unpaired electron with the copper nucleus (I=3/2). The observation of the EPR signal at g=4 together with the usual signal in the g=2 region is consistent with the presence of two magnetically coupled copper(II) centres. These results are indicative that the three ligands strongly bind copper(II) and that ligands T1 and T2 form binuclear copper species in which the two copper(II) centres are close enough

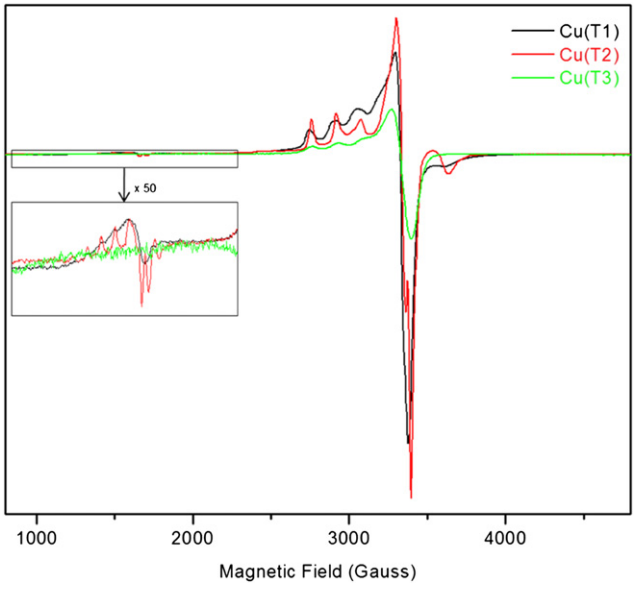

Fig. 5. EPR spectra of the copper(II) complexes of ligands **T1**, **T2** and **T3** obtained in DMSO at 20 K.

to interact. The spectra of copper complexes with T1 and T2 are very similar to that observed for a copper(II) complex of guanine [13] in which X-ray data confirm the structure of binuclear complexes with two copper centres ca. 4 Å apart. The formation of binuclear species for ligand **T3** is not ruled out but in this case the two copper centres must be further distant as their magnetic interaction is not detected by EPR. These results provide evidence for the different flexibility of the ligands, which is introduced by the two different platforms used to anchor the 3,4-HPO units. A full characterization of the structure of the various types of complexes formed by ligands **T1**, **T2** and **T3** is under analysis and due to its complexity will be discussed in a different work.

3. Conclusion

Three novel 3-hydroxy-4-pyridinone based tetradentate ligands have been synthesized and characterized. The ligands exhibit different flexibility that was achieved by the use of two different anchor molecules and pyridinone arms of diverse length. The synthetic versatility of the 3,4-HPO ligands allowed the synthesis of the tetradentate ligands without changing the acid–base properties of the dissociable groups of the pyridinone units thus providing ligands that maintain a high affinity towards metal ions.

Owing to the variety of species formed by metal ions with ligands **T1** and **T2** and to the low solubility of complexes of **T3** we believe that their Zn(II) and VO(II) complexes will not be useful as anti-diabetic agents. However from the structural point of view these ligands have a very rich coordination chemistry, which will be further explored.

4. Experimental section

4.1. General information

Reagents and solvents were purchased as reagent-grade and used without further purification unless otherwise stated. NMR spectra were recorded with Bruker Avance III 400 spectrometer (400.15 MHz for ^{1}H and 100.63 MHz for ^{13}C). Chemical shifts (δ) are reported in parts per million and coupling constants (J) in hertz; internal standard was TMS. Unequivocal ^{1}H assignments were made with aid of 2D gCOSY (^{1}H/^{1}H), while ^{13}C assignments were made on the basis of 2D gHSQC (^{1}H/^{13}C) and gHMBC experiments (delay for long range J C/H couplings were optimized for 7 Hz). Mass spectra were acquired by Unidade De Espectrometria De Masas of Santiago de Compostela and microanalyses were acquired by Unidad De Análisis Elemental of Santiago de Compostela. Flash chromatography was carried out using silica gel Merck (230–400 mesh).

4.2. Synthesis

3-Benzyloxy-2-methyl-4-pyrone and 3-benzyloxy-1-(3′-carboxypropyl)-2-methyl-4-pyridinone was prepared as described in the literature.[14]

4.3. Synthesis of 1,4-bis[(3-benzyloxy-2-methyl-4-pyridinone)propyl]piperazine (1)

(a) Using standard conditions: To a mixture of 1,4-bis(3-aminopropyl)piperazine (5.30 mL, 2.57 mmol), 3-benzyloxy-2-methyl-4-pyrone (1.17 g, 5.41 mmol, 2.1 equiv), ethanol (100 mL) and water (100 mL) was added dropwise a concentrated solution of NaOH until pH 13. The resulting mixture was refluxed during 24 h. After that time, the reaction mixture was concentrated in the rotative evaporator until remove 100 mL of solvent. Subsequently, 100 mL of water was added and the pH was adjusted to 2 using HCl. The aqueous layer was extracted three times with ethyl ether and the organic layer was rejected. The pH of the aqueous layer was adjusted to 10 using a 20% solution of NaOH and it was extracted two times with dichloromethane. The organic layer was dried over anhydrous Na_2SO_4 and the solvent evaporated in vacuo to give 1.07 g (70% yield) of **1** as a white pallid solid. *(b) Using microwave irradiation*: To a mixture of 1,4-bis(3-aminopropyl)piperazine (2.65 mL, 1.29 mmol), 3-benzyloxy-2-methyl-4-pyrone (0.585 g, 2.71 mmol, 2.1 equiv), ethanol (50 mL) and water (50 mL) was added dropwise a concentrated solution of NaOH until pH 13. The resulting mixture was placed in the cavity of a CEM microwave reactor using open vessel conditions. The reaction vial was irradiated at 50 °C (1 min ramp to 50 °C and 30 min hold at 50 °C, using 100 W maximum power). The reaction work-up was similar to the described before affording 0.2517 g of compound **1** (33% yield). ^{1}H NMR (400.15 MHz, DMSO-d_6) δ: 1.71–1.75 (4H, m, 2×CH_2), 2.18 (6H, s, 2×CH_3), 2.20–2.35 (8H, m, 4×CH_2-piperazine), 3.87 (4H, t, *J* 6.8 Hz, 2×CH_2), 5.02 (4H, s, 2×$CH_2C_6H_5$), 6.13 (2H, d, *J* 7.5 Hz, 2×5-H), 7.29–7.40 (10H, m, 2×$CH_2C_6H_5$), 7.58 (2H, d, *J* 7.5 Hz, 2×6-H) ppm.

4.4. Synthesis of 1,4-bis[(3-hydroxy-2-methyl-4-pyridinone) propyl]piperazine (T1)

A 1 M solution of boron trichloride in dichloromethane (16 mL) was dropped slowly into an ice-bath-cooled suspension of **1** (1.60 g, 2.68 mmol) in dry dichloromethane (100 mL), under argon atmosphere. The mixture was stirred at room temperature overnight. Methanol (50 mL) was added to quench the reaction. After removal of the solvent in vacuo, the residue was precipitated with methanol/acetone to afford the hydrochloride salt of **T1** (1.13 g, 75% yield) as a white solid. C, 40.75; N, 8.54; H, 7.12. $C_{22}H_{32}N_4O_4\cdot 4HCl\cdot 5H_2O$ requires C, 40.50; N, 8.59; H, 7.11%. ^{1}H NMR (400.15 MHz, D_2O) δ: 2.18–2.22 (4H, m, 2×CH_2), 2.47 (6H, s, 2×CH_3), 3.21–3.26 (4H, m, 2×CH_2), 3.47–3.56 (8H, m, 4×CH_2-piperazine), 4.31 (4H, t, *J* 7.6 Hz, 2×CH_2), 6.70 (2H, d, *J* 6.8 Hz, 2×5-H), 7.93 (2H, d, *J* 6.8 Hz, 2×6-H). ^{13}C NMR (100.63 MHz, D_2O) δ: 12.3 (CH_3), 24.4 (CH_2), 49.1 (CH_2-piperazine), 53.0 (CH_2), 53.2 (CH_2), 111.3 (C-5), 138.5 (C-6), 142.3 and 142.9 (C-2 and C-3), 159.1 (C-4). MS (FAB) *m*/*z*: 417 $[(M+H)-4HCl]^+$.

4.5. Synthesis of 1,4-bis[(*N*-propanamide-3-benzyloxy-2-methyl-4-pyridinone)propyl]piperazine (2)

(a) Using standard conditions: A mixture of 3-benzyloxy-1-(3′-carboxypropyl)-2-methyl-4-pyridinone (2.57 g, 8.94 mmol, 2.3 equiv), DCC (1.92 g, 9.33 mmol, 2.4 equiv), HOBt (1.26 g, 9.33 mmol, 2.4 equiv) and dry DMF (80 mL) was stirred at room temperature, under argon atmosphere, for 30 min. After that time, 1,4-bis(3-aminopropyl)piperazine (0.80 mL, 3.89 mmol) was added and the resulting reaction mixture was allowed to stir at room temperature for 4 days. Upon filtration and removal of the solvent under reduced pressure, the residue was purified by column chromatography using a mixture of chloroform/methanol (6:4) as eluent to afford 1.87 g (65% yield) of **2** as a white solid. *(b) Using microwave irradiation:* A mixture of 3-benzyloxy-1-(30-carboxypropyl)-2-methyl-4-pyridinone (0.184 g, 0.64mmol, 2.3 equiv), DCC (0.138 g, 0.67mmol, 2.4 equiv), HOBt (90.0mg, 0.67mmol, 2.4 equiv), 1,4-bis(3-aminopropyl)piperazine (0.06mL, 0.28mmol)anddryDMF (20mL) was prepared and placed in the cavity of a CEM microwave reactor using open vessel conditions. The reaction vial was irradiated at 50 °C (1 min ramp to 50 °C and 30 min hold at 50 °C, using 100 W maximum power). The reaction mixture was then purified by column chromatography using a mixture of chloroform/methanol (6:4) as eluent to give **2** (0.113 g, 55% yield). ^{1}H NMR (400.15 MHz, DMSO-d_6) δ: 1.46 (4H, quintet, *J* 6.9 Hz, 2×CH_2), 2.15–2.35 (12H, m, 6×CH_2), 2.21 (6H, s, 2×CH_3), 2.46 (4H, t, *J* 6.8 Hz, CH_2), 2.98–3.05 (4H, m, CH_2), 4.09 (4H, t, *J* 6.8 Hz, 2×CH_2), 5.00 (4H, s, 2×$CH_2C_6H_5$), 6.11 (2H, d, *J* 7.6 Hz, 2×5-H), 7.31–7.43 (10H, m, 2×$CH_2C_6H_5$), 7.51 (2H, d, *J* 7.6 Hz, 2×6-H), 7.96 (2H, t, *J* 5.4 Hz, 2×NH) ppm.

4.6. Synthesis of 1,4-bis[(*N*-propanamide-3-hydroxy-2-methyl-4-pyridinone)propyl]piperazine (T2)

A 1 M solution of boron trichloride in dichloromethane (6 mL) was dropped slowly into an ice-bath-cooled suspension of solution of **2** (0.73 g, 1.00 mmol) in dry dichloromethane (50 mL), under argon atmosphere. The mixture was stirred at room temperature overnight. Methanol (25 mL) was added to quench the reaction. After removal of the solvent, the residue was precipitated with methanol/acetone to afford the hydrochloride salt of **T2** (0.55 g, 78% yield) as a white solid. C, 45.97; N, 11.05; H, 6.78. $C_{28}H_{42}N_6O_6\cdot 4HCl\cdot 2H_2O$ requires C, 45.41; N, 11.35; H 6.81%. ^{1}H NMR (400.15 MHz, D_2O) δ: 1.84–1.90 (4H, m, 2×CH_2), 2.54 (6H, s, 2×CH_3), 2.79 (4H, t, *J* 6.8 Hz, 2×CH_2), 3.15–3.22 (8H, m, 4×CH_2), 3.55–3.65 (8H, m, 4×CH_2-piperazine), 4.56 (4H, t, *J* 6.8 Hz, 2×CH_2), 7.04 (2H, d, *J* 7.2 Hz, 2×5-H), 7.97 (2H, d, *J* 7.2 Hz, 2×6-H) ppm. ^{13}C NMR (100.63 MHz, D_2O) δ: 12.3 (CH_3), 23.4 (CH_2), 35.5 (CH_2), 36.1 (CH_2), 48.7 (CH_2-piperazine), 52.4 (CH_2), 54.5 (CH_2), 111.0 (C-5), 138.7 (C-6), 142.3 (C-2), 142.7 (C-3), 159.1 (C-4), 171.8 (C=O) ppm. MS (FAB) *m*/*z*: 559 $[(M+H)-4HCl]^+$.

4.7. Synthesis of 1,2-bis(*N*-propanamide-3-benzyloxy-2-methyl-4-pyridinone)benzene 3

(a) Using standard conditions: A mixture of 3-benzyloxy-1-(3′-carboxypropyl)-2-methyl-4-pyridinone (0.92 g, 3.19 mmol, 2.3 equiv), DCC (0.69 g, 3.33 mmol, 2.4 equiv), HOBt (0.45 g, 3.33 mmol, 2.4 equiv) and dry DMF (20 mL) was stirred at room temperature, under argon atmosphere, for 30 min. After that time, 1,2-diaminobenzene (0.15 g, 1.39 mmol) was added and the resulting reaction mixture was allowed to stir at room temperature for 3 days. Upon filtration and removal of the solvent under reduced pressure, the residue was purified by flash chromatography using a mixture of chloroform/methanol/ethyl acetate (17:2:1) as eluent to afford **3** (0.31 g, 34% yield) as a white solid. *(b) Using microwave irradiation:* A mixture of 3-benzyloxy-1-(3′-carboxypropyl)-2-methyl-4-pyridinone (0.184 g, 0.64 mmol, 2.3 equiv), DCC (0.138 g, 0.67 mmol, 2.4 equiv), HOBt (90.0 mg, 0.67 mmol, 2.4 equiv), 1,2-diaminobenzene (30.0 mg, 0.28 mmol) and dry DMA (4 mL) was placed in a 10 mL reaction vial, which was then closed under argon atmosphere and placed in the cavity of a CEM microwave reactor. The reaction vial was irradiated at 50 °C (1 min ramp to 50 °C and 30 min hold at 50 °C, using 100 W maximum power). The reaction mixture was then purified by flash chromatography (chloroform/

methanol/ethyl acetate in 17:2:1) to give **3** (54.3 mg, 30% yield). C, 60.57; N, 7.64; H, 5.60. $C_{38}H_{38}N_4O_6\cdot CHCl_3\cdot 1/2H_2O$ requires C, 60.43; N, 7.23; H, 5.20%. ^{1}H NMR (400.15 MHz, DMSO-d_6) δ: 2.25 (6H, s, 2×CH_3), 2.73 (4H, t, *J* 6.9 Hz, 2×CH_2), 4.18 (4H, t, *J* 6.9 Hz, 2×CH_2), 5.01 (4H, s, 2×C$H_2C_6H_5$), 6.15 (2H, d, *J* 7.5 Hz, 2×5-H), 7.13–7.15, 7.31–7.42 and 7.46–7.48 (14H, 3 m, Ar–H), 7.61 (2H, d, *J* 7.5 Hz, 2×6-H), 9.41 (2H, br s, 2×NH) ppm. ^{13}C NMR (100.63 MHz, DMSO-d_6) δ: 11.9 (CH_3), 36.6 (CH_2), 48.9 (CH_2), 71.8 ($CH_2C_6H_5$), 116.0, 125.0, 127.8, 128.2, 128.3, 130.1, 137.8, 139.5, 140.5, 145.3, 168.3, 171.9 ppm. MS (FAB$^+$) *m/z:* 647 (M+H)$^+$.

4.8. Synthesis of 1,2-bis(*N*-propanamide-3-hydroxy-2-methyl-4-pyridinone)benzene T3

A 1 M solution of boron trichloride in dichloromethane (2.7 mL) was dropped slowly into an ice-bath-cooled suspension of solution of **3** (0.30 g, 0.46 mmol) in dry dichloromethane (17 mL), under argon atmosphere. The mixture was stirred at room temperature overnight. Methanol (5 mL) was added to quench the reaction mixture. After removal of the solvent, the residue was precipitated with methanol/acetone to afford quantitatively hydrochloride salt of **T3** as a white powder. C, 51.86; N, 10.04; H, 5.56. $C_{24}H_{26}N_4O_6\cdot 2HCl\cdot H_2O$ requires C, 51.71; N, 10.05; H, 5.42%. ^{1}H NMR (400.15 MHz, DMSO-d_6) δ: 2.63 (6H, s, 2×CH_3), 3.05 (4H, t, *J* 6.8 Hz, 2×CH_2), 4.66 (4H, t, *J* 6.8 Hz, 2×CH_2), 7.09–7.12 (2H, m, Ar–H), 7.31 (2H, d, *J* 7.0 Hz, 2×5-H), 7.55–7.57 (2H, m, Ar–H), 8.28 (2H, d, *J* 7.0 Hz, 2×6-H), 10.12 (2H, s, NH) ppm. ^{13}C NMR (100.63 MHz, DMSO-d_6) δ: 12.6 (CH_3), 35.9 (CH_2), 52.4 (CH_2), 110.6 (C-5), 124.5, 124.6, 129.6, 138.5 (C-6), 141.8, 142.8, 158.5 (C-4), 167.7 (C=O) ppm.

4.9. Single-crystal X-ray diffraction

Single-crystals of $2[C_{24}H_4N_{24}O_4]4Cl\cdot 6(H_2O)\cdot C_6H_{14}$, 2(**T3**) $4Cl\cdot 6(H_2O)\cdot C_6H_{14}$ were harvested from the crystallization vial and immersed in highly viscous FOMBLIN Y perfluoropolyether vacuum oil (LVAC 140/13). A suitable single-crystal was mounted on a Hampton Research CryoLoop with the help of a Stemi 2000 stereomicroscope equipped with Carl Zeiss lenses.[15] Data were collected on a Bruker X8 Kappa APEX II charge-coupled device (CCD) area-detector diffractometer (Mo Kα graphite-monochromated radiation, λ=0.71073 Å) controlled by the APEX2 software package,[16] and equipped with an Oxford Cryosystems Series 700 cryostream monitored remotely using the software interface Cryopad.[17] Images were processed using the software package SAINT+,[18] and data were corrected for absorption by the multi-scan semi-empirical method implemented in SADABS.[19] The structure was solved by direct methods implemented in SHELXS-97,[20,21] and refined from successive full-matrix least-squares cycles on *F2* using SHELXL-97.[20,22] All non-hydrogen atoms were successfully refined using anisotropic displacement parameters, including those from the crystallization solvent molecules (water and *n*-hexane).

Hydrogen atoms associated with the amine (N–H) and hydroxyl (O–H) groups of **T3** were markedly visible in difference Fourier maps and were included in the structure with the N–H and O–H distances restrained to 0.85(1) and 0.90(1) Å, respectively, and with U_{iso} fixed at 1.5×U_{eq} of the parent attached atom. H-atoms bound to carbon were located at their idealized positions using appropriate *HFIX* instructions in SHELXL: *43* for the aromatic, *23* for the –CH_2 carbons and *137* for the terminal –CH_3 methyl groups. All these atoms were included in subsequent refinement cycles in riding-motion approximation with isotropic thermal displacements parameters (U_{iso}) fixed at 1.2 or 1.5×U_{eq} of the carbon atom to which they are attached. The H-atoms associated with the crystallization water molecules were clearly visible in the difference Fourier maps and included in the final structure model during subsequent refinement stages with the O–H and H···H distances restrained to 0.90(1) and 1.50(1) Å, respectively. This procedure ensures a chemically reasonable geometry for these molecules. Atoms were treated using a riding-motion approximation with an isotropic thermal displacement parameter (U_{iso}) fixed at 1.5×U_{eq} of the parent oxygen atom. Despite the H-atoms of the *n*-hexane molecule were not located in the refined structure, they have been included in the empirical formula of the compound.

Information concerning the crystallographic data collection and structure refinement of **T3**: Formula, $C_{27}H_{41}Cl_2N_4O_5$; M_r=636.54; crystal size 0.21×0.10×0.06 mm^3, *T*=150(2) K; Monoclinic; space group $P2_1/n$; *a*=9.9479(9) Å, *b*=23.770(2) Å, *c*=12.4952(11) Å; β=105.412(4)°; *V*=2848.4(5) Å^3; *Z*=4; ρ_{calcd}=1.468 g cm^{-3}; μ=0.289 mm^{-1}; 45,929 reflections collected, 5827 independent reflections, R_{int}=0.0503; *R*1=0.0570 and *wR*2=0.1523 for data $I>2\sigma(I)$; *R*1=0.0800 and *wR*2=0.1682 for all data.

Crystallographic data (excluding structure factors) for the structure in this paper have been deposited with the Cambridge Crystallographic Data Centre as supplementary publication no. CCDC-811973. Copies of the data can be obtained, free of charge, on application to CCDC, 12 Union Road, Cambridge CB2 1EZ, UK (fax: +44 (0)1223 336033 or e-mail: deposit@ccdc.cam.ac.uk).

4.10. Potentiometric and spectrophotometric determinations

All solutions were prepared with double de-ionized water (conductivity less than 0.1 μS cm^{-1}). Potentiometric measurements were performed with a Crison 2002 decimillivoltmeter and a Crison 2031 automatic burette controlled by an IBM 425SX computer. The electrode assembly consisted of a Russell 900029/4 double junction Ag/AgCl reference electrode and a Russell 18026/02 glass electrode as indicator. All titrations were carried out in a thermostat-controlled double-walled glass cell at (25.0±0.1 °C) under argon atmosphere, homogeneity of the solutions was maintained using a Crison 2038 magnetic stirrer and ionic strength was adjusted to 0.10 M with NaCl. Solutions of NaOH were prepared in de-ionized water previously purged with argon while boiling to reduce carbonate impurity. System calibration was performed by the Gran method[23] in terms of hydrogen ion concentration by titrating solutions of strong acid with strong base. Before each run a calibration was performed to check the electrode behaviour. For the determination of the acid dissociation constants of the ligands an aqueous solution (1 mM, *I*=0.1 M NaCl) of the protonated ligand was titrated with NaOH (ca. 0.03 M, 25.0±0.1 °C) under an argon atmosphere.

For the spectroscopic data the pH values were measured by a Crison pH meter Basic 20+, which is equipped with a combined glass electrode, and it was standardized at 25 °C by using standard buffers of pH 4, 7 and 9. The UV–vis spectra obtained to determine absorptiometric pK_a values were record, at each pH, using a Varian Cary bio50 double beam spectrophotometer, equipped with a Varian Cary single cell Peltier accessory controlled by a computer. Stock solutions of the ligands were prepared in water (*I*=0.1 M NaCl). After each pH adjustment the solution was transferred into the cuvette, and the absorption spectra were recorded. Spectra were acquired at 25 °C and between 200 and 400 nm (1 nm resolution).

The pK_a values were determinate by using the programs: Hyperquad 2006 for the treatment of the curves obtained in potentiometric titration and HypSpec for the treatment of the obtained UV–vis spectra.[24] The errors associated were determined using the Albert and Sergeant theory.[25] The species distribution curves were plotted with the HySS program.

4.11. UV–vis spectroscopy

Electronic absorption spectra of solutions of the complexes were recorded with a Varian Cary bio50 spectrophotometer, equipped with a Varian Cary single cell Peltier accessory. Spectra were

recorded at 25 °C in 1 cm path length quartz cells with a slit width of 1 nm, in the range 200–800 nm. The samples were prepared by dissolution of the compound in dried DMSO and placed in the quartz cells. Typical solution concentrations were in the range 1×10^{-5} to 1×10^{-6} M.

4.12. EPR spectroscopy

EPR spectra of the paramagnetic complexes were recorded in frozen solution in the temperature range 20–77 K using an X-band (9 GHz) Brucker EMX spectrometer equipped with a variable temperature unit (Oxford ESR900). The samples were prepared by dissolution of the compound in dried DMSO and placed in quartz tubes.

Acknowledgements

Financial support from FCT through project PTDC/QUI/67915/2006 is gratefully acknowledged. A.L. (SFRH/BD/30083/2006) thanks FCT for PhD grant. We also thank Dr. Andrea Carneiro from CENTI, V.N. Famalicão, for making available a CEM Discover microwave reactor. The Bruker Avance II 400 spectrometer is part of the National NMR network and was purchased under the framework of the National Programme for Scientific Re-equipment, contract REDE/1517/RMN/2005, with funds from POCI 2010 (FEDER) and (FCT).

Supplementary data

Supplementary data associated with this article can be found in the online version, at doi:10.1016/j.tet.2011.04.035. These data include MOL files and InChIKeys of the most important compounds described in this article.

References and notes

1. (a) Burgess, B.; Rangel, M. *Adv. Inorg. Chem.* **2008**, *60*, 167; (b) Santos, M. A. *Coord. Chem. Rev.* **2008**, *252*, 1213.
2. (a) Nunes, A.; Podinovskaia, M.; Leite, A.; Gameiro, P.; Zhou, T.; Ma, Y.; Kong, X.; Schaible, U. E.; Hider, R. C.; Rangel, M. *J. Biol. Inorg. Chem.* **2010**, *15*, 861; (b) Ma, Y. M.; Hider, R. C. *Bioorg. Med. Chem.* **2009**, *17*, 8093.
3. Esteves, M. A.; Cachudo, A.; Chaves, S.; Santos, M. A. *Eur. J. Inorg. Chem.* **2005**, 597–605.
4. (a) Harrington, J. M.; Chittamuru, S.; Dhungana, S.; Jacobs, H. K.; Gopalan, A. S.; Crumbliss, A. L. *Inorg. Chem.* **2010**, *49*, 8208; (b) Lambert, T. N.; Chittamuru, S.; Jacobs, H. K.; Gopalan, A. S. *Tetrahedron Lett.* **2002**, *43*, 7379.
5. Tei, L.; Baranyai, Z.; Brücher, E.; Cassino, C.; Demicheli, F.; Masciocchi, N.; Giovenzana, G. B.; Botta, M. *Inorg. Chem.* **2010**, *49*, 616.
6. (a) Niu, Y.; Hou, H.; Wei, Y.; Fan, Y.; Zhu, Y.; Du, C.; Xin, X. *Inorg. Chem. Commun.* **2001**, *4*, 358; (b) Li, G.; Lü, J.; Li, X.; Yang, H.; Xu, B.; Cao, R. *CrystEngComm* **2010**, *12*, 3780; (c) Hsu, S.-C.; Wu, J.-Y.; Lee, C.-F.; Lee, C.-C.; Lai, L.-L.; Lu, K.-L. *CrystEngComm* **2010**, *12*, 3388.
7. Chaves, S.; Marques, S. M.; Matos, A. M. F.; Nunes, A.; Gano, L.; Tuccinardi, T.; Martinelli, A.; Santos, M. A. *Chem.—Eur. J.* **2010**, *16*, 10535.
8. For microwave heating reviews see: (a) Caddick, S.; Fitzmaurice, R. *Tetrahedron* **2009**, *65*, 3325; (c) Kappe, C. O.; Dallinger, D. *Mol. Divers.* **2009**, *13*, 71; (d) Polshettiwar, V.; Varma, R. S. *Chem. Soc. Rev.* **2008**, *37*, 1546; (e) Kappe, C. O. *Chem. Soc. Rev.* **2008**, *37*, 1127; (f) Dallinger, D.; Kappe, C. O. *Chem. Rev.* **2007**, *127*, 2563; (g) Nüchter, M.; Ondruschka, B.; Bonrath, W.; Gum, A. *Green Chem.* **2004**, *6*, 128; (h) Kappe, C. O. *Angew. Chem., Int. Ed.* **2004**, *43*, 6250.
9. For recent examples see: (a) Di Credico, B.; Reginato, G.; Gonsalvi, L.; Peruzzini, M.; Rossin, A. *Tetrahedron* **2011**, *67*, 267; (b) Silva, A. M. G.; Leite, A.; Andrade, M.; Gameiro, P.; Brandão, P.; Felix, V.; de Castro, B.; Rangel, M. *Tetrahedron* **2010**, *66*, 8544; (c) Tang, D.; Buck, J. R.; Hight, M. R.; Manning, H. C. *Tetrahedron Lett.* **2010**, *51*, 4595; (d) Allam, A.; Behr, J.-B.; Dupont, L.; Nardello-Rataj, V.; Plantier-Royon, R. *Carbohydr. Res.* **2010**, *345*, 731; (e) Zhang, S.-H.; Feng, C. *J. Mol. Struct.* **2010**, *977*, 62; (f) Lee, Y. S.; Fernandes, S.; Kulkarani, V.; Mayorov, A.; Davis, P.; Ma, S.-w.; Brown, K.; Gillies, R. J.; Lai, J.; Porreca, F.; Hruby, V. J. *Bioorg. Med. Chem. Lett.* **2010**, *20*, 4080; (g) Farruggia, G.; Iotti, S.; Lombardo, M.; Marraccini, C.; Petruzziello, D.; Prodi, L.; Sgarzi, M.; Trombini, C.; Zaccheroni, N. *J. Org. Chem.* **2010**, *75*, 6275; (h) Goldys, A.; McErlean, C. S. P. *Tetrahedron Lett.* **2009**, *50*, 3985; (i) Pimentel, L. C. F.; de Souza, A. L. F.; Fernández, T. L.; Wardella, J. L.; Antunes, O. A. C. *Tetrahedron Lett.* **2007**, *48*, 831.
10. Dega-Szafran, Z.; Jaskólski, M.; Kurzyca, I.; Barczyński, P.; Szafran, M. *J. Mol. Struct.* **2002**, *614*, 23.
11. Queiros, C.; Amorim, M. J.; Leite, A.; Ferreira, M.; Gameiro, P.; de Castro, B.; Biernacki, K.; Magalhães, A.; Burgess, J.; Rangel, M. *Eur. J. Inorg. Chem.* **2011**, 131.
12. Rangel, M.; Leite, A.; Amorim, M. J.; Garriba, E.; Micera, G.; Lodyga-Chruscinska, E. *Inorg. Chem.* **2006**, *45*, 8086.
13. Li, L.; Murthy, N. N.; Telser, J.; Zakharov, L. N.; Yap, G. P. A.; Rheingold, A. L.; Karlin, K. D.; Rokita, S. E. *Inorg. Chem.* **2006**, *45*, 7144.
14. Santos, M. A.; Gil, M.; Marques, S.; Gano, L.; Cantinho, G.; Chaves, S. *J. Inorg. Biochem.* **2002**, *92*, 43.
15. Kottke, T.; Stalke, D. *J. Appl. Crystallogr.* **1993**, *26*, 615–619.
16. *APEX2. Data Collection Software Version 2.1-RC13*; Bruker AXS: Delft, The Netherlands, 2006.
17. *Cryopad. Remote Monitoring and Control, Version 1.451*; Oxford Cryosystems: Oxford, United Kingdom, 2006.
18. *SAINT+. Data Integration Engine v. 7.23a*©; Bruker AXS: Madison, WI, USA, 1997–2005.
19. Sheldrick, G. M. *SADABS v.2.01, Bruker/Siemens Area Detector Absorption Correction Program*; Bruker AXS: Madison, WI, USA, 1998.
20. Sheldrick, G. M. *Acta Crystallogr. A* **2008**, *64*, 112–122.
21. Sheldrick, G. M. *SHELXS-97, Program for Crystal Structure Solution*; University of Göttingen: Göttingen, 1997.
22. Sheldrick, G. M. *SHELXL-97, Program for Crystal Structure Refinement*; University of Göttingen: Göttingen, 1997.
23. (a) Gran, G. *Analyst* **1952**, *77*, 661–671; (b) Rossotti, F.; Rossotti, H. *J. Chem. Educ.* **1965**, *42*, 375.
24. Gans, P.; Sabatini, A.; Vacca, A. *Talanta* **1996**, *43*, 1739.
25. Albert, A.; Sergeant, E. P. *The Determination of Ionization Constants*, 2nd ed.; Chapman & Hall: London, 1971.